

Electron emission under uniform magnetic field of conductor materials used for spatial and fusion applications.

Nicolas Fil, Mohamed Belhaj, Julien Hillairet, Jerome Puech, Renaud Mathevet

▶ To cite this version:

Nicolas Fil, Mohamed Belhaj, Julien Hillairet, Jerome Puech, Renaud Mathevet. Electron emission under uniform magnetic field of conductor materials used for spatial and fusion applications.. INTERNATIONAL WORKSHOP ON MULTIPACTOR, CORONA AND PASSIVE INTERMODULATION (MULCOPIM 2017) MULCOPIM 2017, Apr 2017, NOORDWIJK, Netherlands. hal-03746652

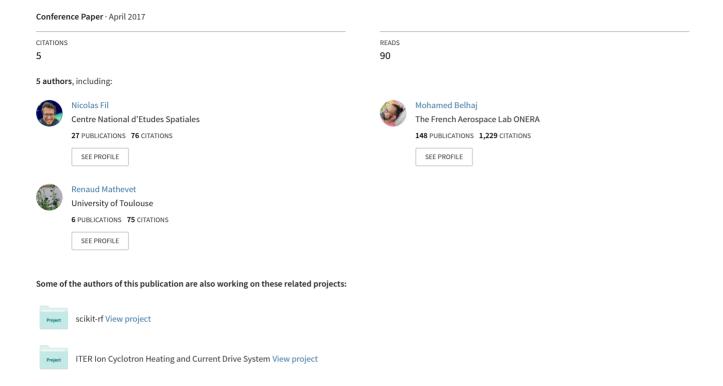
HAL Id: hal-03746652 https://hal.science/hal-03746652v1

Submitted on 23 Aug 2022

HAL is a multi-disciplinary open access archive for the deposit and dissemination of scientific research documents, whether they are published or not. The documents may come from teaching and research institutions in France or abroad, or from public or private research centers.

L'archive ouverte pluridisciplinaire **HAL**, est destinée au dépôt et à la diffusion de documents scientifiques de niveau recherche, publiés ou non, émanant des établissements d'enseignement et de recherche français ou étrangers, des laboratoires publics ou privés.

Electron emission under uniform magnetic field of conductor materials used for spatial and fusion applications.



Electron emission under uniform magnetic field of conductor materials used for spatial and fusion applications.

Nicolas Fil (1) (2) (3), Mohamed Belhaj (2), Julien Hillairet (1), Jérôme Puech (3), Renaud Mathevet (4)

(1) CEA-The French Alternative Energies and Atomic Energy Commission CEA Cadarache, DRF//IRFM/SI2P/GSCP, 13108 Saint Paul-Lez-Durance, France

⁽²⁾ ONERA-The French Aerospace Lab ONERA, 31055, France

(3) CNES-The French National Centre for Space Studies CNES, DCT/RF/HT, 31000 Toulouse, France

(4) LNCMI, Intense Magnetic Fields Laboratory 31400 Toulouse, France

INTRODUCTION

The multipactor effect can decrease the performance of Radio-Frequency (RF) systems functioning under vacuum. Multipactor is a resonance effect between the RF electric field and the motion of the electrons [1]. It highly depends on the electron emission properties of the RF component materials. Applications using these kind of components are telecommunication satellite [2], fusion experimental reactors with Tokamak [3] or particle accelerators [4] among others. Many experimental [5] and theoretical [6]–[9] works have been conducted to study this undesirable phenomenon. The aim of these approaches is to determine the multipactor power threshold. Above this threshold, multipactor can appears and damage RF systems.

In some applications concerned by the multipactor effect, RF components are submitted to DC magnetic fields. For instance, in telecommunication satellite, magnetic fields of a few tenths of Tesla produced with permanent magnets are used in circulators and isolators. In fusion reactors, rectangular copper waveguides are located under intense magnetic fields of few Tesla generated by toroidal and poloidal coils. Multipactor simulations codes are used to calculate the threshold that would trigger the electron density growth by following the electrons under the RF wave electromagnetic field [7], [8]. Multipactor modeling can also take into account an external magnetic field. It induces gyratory motions of electrons within the simulated RF structure. Studies have been made on the effect of external magnetic field on multipactor discharge [10]. However, to our knowledge, there are no multipactor simulation codes which take into account the influence of DC magnetic field on the electron emission process.

In this paper we will often speak about incident, primary, secondary and backscattered electrons. Here we specify the definitions and nomenclature. Incident electron (IE) is electron which impacts a material surface. At this impact, IE can penetrate the material and then transfer a part of its energy through inelastic interactions. The IE can excite inner material electron which could escape the material surface [11]: in this case the electron emitted is called secondary electron (SE). The IE can also escape the surface material due to several inelastic and elastic interactions: in this case the electron emitted is called backscattered electrons (BSE). Primary electron (PE) term is used to define all the electrons generated by an electron gun. Experimentally, an electron gun is used to provide a quasi mono-energetic primary electron beam. We commonly define the Total Electron Emission Yield (TEEY, σ) which is the number of the whole electrons emitted by the surface material divided by the number of IE.

To study the effect of the magnetic field on the Total Electron Emission Yield (TEEY), a new experimental setup has been developed. The measurement of the TEEY under magnetic field is challenging since the magnetic field affects the trajectory of the electrons. A special attention to the design of the experimental setup and to the choice of the measurement methodology has been taken to circumvent the possible artefacts that are related to the high sensitivity of incoming and emitted electrons trajectories to the DC magnetic field. In this paper, the new developed experimental setup and the measurement methods are described in details. Thereafter, the validation procedure of the TEEY measurement methodology based on both experiments and modeling with SPIS code [12] is given. TEEY measurements on copper under a normal DC magnetic field are also presented. In the last section we give the works under investigation which continue our study of the influence of the DC magnetic field on electron emission properties.

A NEWLY EXPERIMENTAL SETUP

The experimental setup presented hereafter aims to measure TEEY with magnetic field. First we introduce the setup and its operation. Then we explain the validation procedure that has been made with the help of both measurements and modeling.

Description

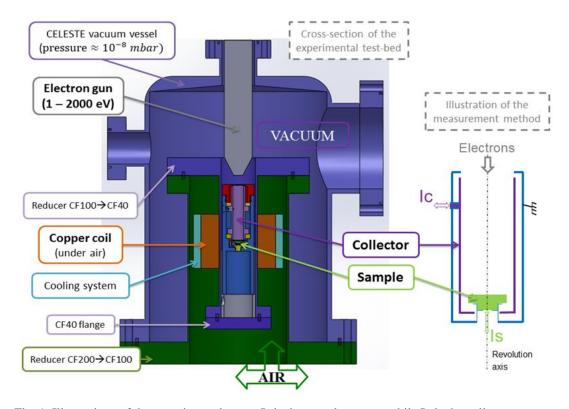


Fig. 1. Illustrations of the experimental setup. I_S is the sample current while I_C is the collector current.

We use an available vacuum chamber of 34 mm³. Working with magnetic field implies to deal with a certain amount of magnetic energy. To obtain the higher magnetic field amplitude as possible while using the lowest coil current, we need to work with the smallest coil as possible. We also need to avoid outgassing in vacuum, so the coil has been placed outside the vacuum vessel, as close as possible to the sample (see the two reducers on Fig. 1). A 41 mm-diameter copper coil has then been directly built on the reducer CF100 \rightarrow CF40 tube. A cooling system can be added to prevent overheating of the coil if higher fields are required. The 10 mm-disc sample is located in a 110 mm high cylinder composed of eight pieces with a cylindrical collector. Both are isolated from each other and from the ground. We measure the sample current (I_S) and the collector current (I_C) independently. By connecting the sample and the collector together, the system becomes a Faraday cup, which is used to measure the incident current (I_F).

The sample surface was placed in the plane at the center of the solenoid in the plane perpendicular to its axis in such way that the field was normal to the surface and nearly uniform around the sample (we calculated magnetic field non-uniformity well below 1% across the whole sample). The magnetic field amplitude has been measured along the coil axis thanks to a Gaussmeter and a hall-effect sensor longitudinal probe. A 1 A current on the coil generates an 11.3 mT magnetic field at the sample surface.

The vacuum vessel can reach a pressure of 10⁻⁸ mbar thanks to turbomolecular pump. A 1eV-2keV ELG 2 Kimball Physics electron gun was used to provide a quasi mono-energetic primary electron beam. The output electron gun diaphragm was placed as close as possible to the sample surface to minimize the influence of the magnetic field on the primary electrons trajectories. The electron gun can operate in continuous or pulsed mode. In this paper, all measurements presented have been made in continuous mode. The sample as well as the collector can be independently biased to positive or negative voltage.

Validation with measurements on copper samples

Before studying the influence of the magnetic field on TEEY, the chosen measurement method was validated by measuring the TEEY on copper without DC magnetic field. First, the primary electron current (I_F) was measured by biasing the electrical connected sample and collector at +18V (*faraday cup* configuration). Then the sample was disconnected from the collector and biased to -9V (the collector remains at +18V) and both the sample current (I_S) and the collector current (I_C) were measured. The sample was negatively biased with respect to the collector in order to avoid recollection of secondary or backscattered electrons [13]. This is crucial to get coherent TEEY results: the sample current (I_S) is only due to primary electrons impacts. From I_F , I_S and I_C measurements the yield can be deduced thanks to one of the expressions (1), (2) or (3) below [14].

$$Yield 1: \sigma = \frac{I_c}{I_f} \tag{1}$$

$$Yield 2: \sigma = \frac{I_f - I_s}{I_f}$$
 (2)

$$Yield 3: \sigma = \frac{I_c}{I_c + I_s} \tag{3}$$

According to the current conservation law ($I_F = I_S + I_C$), the quantities defined by the expressions (1), (2) and (3) should be strictly equal. Any difference reflects an error in the measurement of I_c , I_F or I_S [14]. Fig. 2 compares the yields deduced by using the three expressions. Theses TEEY were measured twice to check the result reproducibility. For both set of measures we see similar yields which validate the chosen measurement methodology as well as the experimental setup. The very good agreement observed between measurement 1 and measurement 2 confirms the good reproducibility of the measurements on our experimental test-bed.

When measuring the three currents, the oscilloscope gives us respective absolute uncertainties from which we calculate the statistical error on the yields to be less than 1% for all measurements. The main source of experimental uncertainties comes from the stability of the electron gun power supply, especially from grid and focus tensions. Moreover, the cathode's resistance temperature and the chamber's pressure vary with time. The primary electrons have 0.5eV dispersion in energy set while the conical electron beam has an aperture angle up to 8°. Other experimental errors are coming from evaporation and contamination from both the electron gun and the sample. When we work with a magnetic field, the heat from the coil leads to outgassing from inner materials. Taking all these contributions into account makes the determination of the electron emission measurements uncertainty difficult. It also explains the small discrepancy between Measures 1 and 2 on Fig. 2.

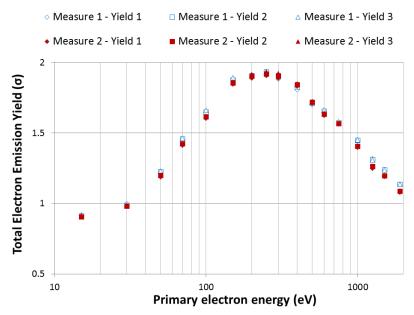


Fig. 2. TEEY measurements on laminate copper sample. Measures 1 and 2 have both three yields calculated from three formulas (1), (2) and (3).

First TEEY measurements under magnetic field

Thanks to the validation presented in the previous section, we can now make TEEY measurements under magnetic field. First we study the current conservation law ($I_F = I_S + I_C$) when a magnetic field is generated. We work with 1A-current on the coil which generates an 11.3 mT magnetic field at the sample surface. We measured the primary electron current (I_F) in faraday cup configuration. Then the sample was disconnected from the collector and biased to -9V (the collector remains at +18V) and both the sample current (I_S) and the collector current (I_C) were measured. Fig. 3 compares the yields deduced by using the three expressions (1), (2) and (3). We see different yield which means that the current conservation law is not verified with an 11.3 mT magnetic field at the sample surface.

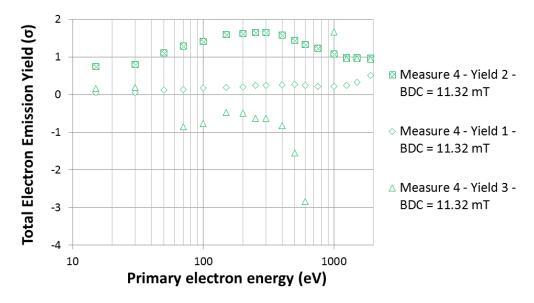


Fig. 3. TEEY measurements under magnetic field perpendicular to the surface laminate copper sample. Measure 4 has been made with an 11.3mT magnetic field at the coil center. The yields are calculated from the three formulas (1), (2) and (3).

The main difficulty in measuring electron emission under a magnetic field comes from electron motions. The effect of a DC magnetic field is to bend the trajectories of charged particles which influences not only the motion of the primary electrons but also secondary and backscattered electrons. We observe during measurements a variation of the primary electron current (I_F) in faraday cup configuration in function of the intensity of the magnetic field while all the others parameters stay constants (voltages of our system, electron gun parameters, oscilloscope settings). We also see variations of the collector current (I_C) when only the magnetic field intensity varies.

To interpret and understand our TEEY measurements under magnetic field, we have thus created a model of our system with SPIS software. In SPIS simulations, we can control the potentials of our system as well as the primary electron beam (angle and energy) and study the trajectories of the three types of electrons (primary, secondary and backscattered) under a homogenous magnetic field.

Test-bed modeling with SPIS software

SPIS (Spacecraft Plasma Interaction System) is a software toolkit for spacecraft-plasma interactions and spacecraft charging modelling [12]. It allows users to model the plasma dynamics (kinetic or fluid, electrostatic or electromagnetic) and its coupling with the spacecraft (equivalent circuit approach). All kinds of environments and systems are supported. SPIS allows us to make simulations with a uniform and a homogenous magnetic field.

We have created a model of our system represented on Fig. 1. The goal is to determine where the primary, secondary and backscattered electrons are collected in function of experimental measurement configuration. Our model is made to get these information for the sample, the collector, the inner flanges (Reducer CF200/CF100+Reducer CF100/CF40+Flange CF40), the sample support, the vacuum vessel and the emission surface of the electron gun. The primary electrons are generated by a surface of π mm² representing the emission surface of the electron gun used in our experimental test-bed. SPIS simulations follow each charged particle. When an electron impacts a surface, SPIS

calculates the response thanks to secondary electron emission models [15]. The emitted electrons (secondary and backscattered) are also followed by the simulation until the next impact. It is important to notice that SE and BSE can also generate SE and BSE from their impacts with materials; these electrons are commonly called tertiary electrons which can also generate SE and BSE and so on. SPIS software follows all the electrons generated and the outputs give the contributions of all SE and BSE. We study on which surface the primary, secondary and backscattered electrons are collected. We made simulations to study the influence of the magnetic field strength on the electrons trajectories. We also investigate the impact of potential and primary electron energy variations. The magnetic field strength has been varied from 0 to 1.132 T while the primary electron energy from 5 to 2000 eV. We have tested many collector potentials (from +9 to +2000 V) while the sample is maintained at -9 V.

The applied DC magnetic field induces a primary electron beam narrowing or widening depending on the magnetic field strength and the primary electron energy. When the magnetic field is under 39.2mT, all primary electrons (from 0 to 2000 eV) are collected by the sample surface. But if we increase the magnetic field strength up to 113.2 mT, primary electrons below than 100eV goes on both sample and collector surfaces while primary electrons of more than 250eV are collected by the sample surface only. At 1.132 T all primary electrons (from 5 to 2000 eV) are collected by the collector, no one reaches the sample. In this last configuration, we cannot measure the sample current (I_S), the experimental setup should be modified to do so.

The emitted electrons (secondary and backscattered) trajectories are also modified: without magnetic field, nearly all the emitted electrons impact the collector but with a magnetic field they escape the system and impact the wall of the vacuum vessel instead impacting the collector. With this SPIS simulation results we find the behavior experimentally observed on Fig. 3; electron escapements explain why the current conservation law is not verify when TEEY is measured under magnetic field. As the consequence, the expressions (1) and (3) lead to lower yields values and we get measurements like those represented on the Fig. 3. We cannot use these two expressions to calculate the TEEY under magnetic field, but the expression (2) is still useful as it is independent of the collector current. There is one necessary condition to use the expression (2): the measure of the sample current (I_S) must be free of electron recollection phenomenon on the sample surface. It means that secondary and backscattered electrons should not be collected by the sample surface. This is verified with SPIS simulation.

This last point is illustrated in Fig. 4 which shows the electrical potential map surrounding the sample: no potential barrier is seen which could make SE or BSE recollected by the sample surface. A clipping plane representing the surface where SE and BSE electrons are collected is also given. The sample is not collecting the SE or BSE electrons.

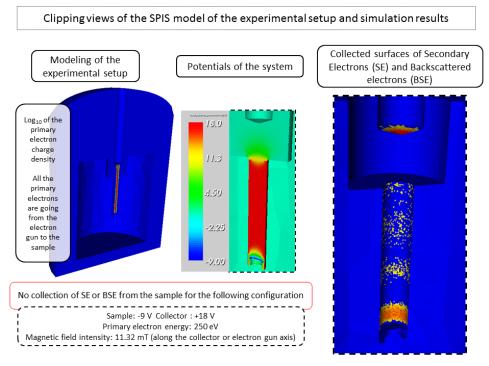


Fig. 4. SPIS modelling of the setup. The whole system is showed on the left while the electrical potential map is represented in the middle. On the right, a clipping plane of the system represents the surface where SE and BSE are collected.

TEEY UNDER MAGNETIC FIELD

After the validation and calibration procedures, TEEY measurements under magnetic field were performed. Each configuration is verified with SPIS simulations. Some results are shown in Fig. 5. For the first two series (measure 1 & 2), no magnetic field has been used while a 4.53 mT and 11.3 mT magnetic field was applied normal to the surface in measures 3 and 4. For all primary electron energies we observe a decrease of the TEEY when the magnetic field was applied. The effect of the field increases with its amplitude. These first results still need further investigations before drawing any final conclusion. We know, thanks to simulations on SPIS, that there no artefact due to the experimental setup. We also observe that 4.53 mT and 11.3 mT magnetic fields induce a primary electron beam narrowing which decreases the sample surface impacted. We then need to study the relation between the magnetic field intensity and the conditionning effect [16] as well as the Dose effect [17].

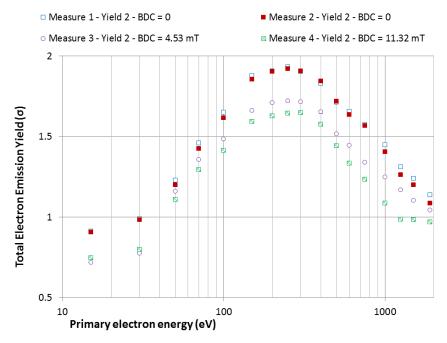


Fig. 5. TEEY measurements on laminate copper sample with and without magnetic field perpendicular to the surface sample

FUTURE WORKS

We are working on making new measurements and modeling with different magnetic field amplitudes as well as different morphology surface samples. We are investigating the correlations between surface morphology and magnetic field amplitude on electron emission intensity. The magnetic field bends electron's trajectories which could make recollections of secondary and backscattered electrons or in contrary help them to escape from sample surface. We can also have conditionning and dose effects due to the magnetic field. These effects are under investigations and depend on the electrons energies, the magnetic field amplitude and the sample morphology surface.

We are making studies which involve both experiments and SPIS modeling. First we want to measure TEEY on polished copper. Many ways to obtain low roughness copper sample is under investigation such as mechanical polishing and electro-polishing. Simulations on SPIS already show no SE and BSE recollections by the sample with and without magnetic field. This kind of samples will give us new information on our experimental setup as well as on conditionning and dose effects.

In a second time, we study specific surface morphologies. We are working on three dimensions periodic morphology surfaces made with rectangular or pyramidal blocks (Fig. 6) [18], [19]. This figure shows SPIS modeling and we want to create some of these surfaces on real samples in order to make TEEY measurements under magnetic field.

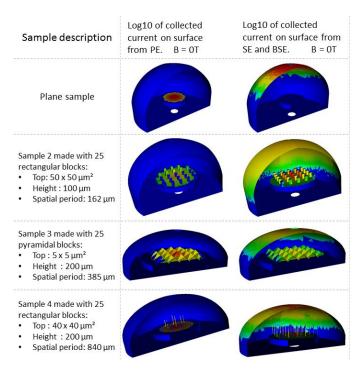


Fig. 6. SPIS modeling of four samples in order to the correlations between surface morphology and magnetic field amplitude on electron emission properties.

First SPIS simulation results show that the plane sample has no recollection of SE and BSE for magnetic field amplitude of 0, 0.0001, 0.001, 0.01, 0.1 and 1 T. For the other three samples, we observe recollection of SE and BSE from the samples. We discern if the electrons are collected by the top surfaces of the blocks, by the lateral surfaces of the blocks or by the surfaces between the blocks. We determine the percentages of PE, SE and BSE collected by each of these surfaces as well as by the sample support surface or by the surrounding surface.

For example if we study the Fig. 6 - sample 4 at PE energy of 250eV, we can make the Table 1. We first see a narrowing of the primary electron beam due to the magnetic field: the percentage of PE collected by the blocks top surfaces increase with the magnetic field amplitude. We also observe an increase of the SE and BSE collection by the blocks lateral surfaces with an increase of the magnetic field intensity. Then the vacuum vessel collected current decreases with the magnetic field intensity which means that the number of electrons emitted by the sample decreases with the magnetic field intensity. This leads to a decrease of the TEEY.

Table 1. Percentages of collected currents from PE, Se and BSE on surfaces of the sample 4 in function of the magnetic field amplitude. SPIS simulations made with primary electron energy of 250eV.

Electron type	Surface definition —	Percentage of collected current on surfaces		
		B = 0 T	B = 0.16 T	B = 1.6 T
Primary Electrons (PE)	Blocks top surfaces	0.4	1.5	1.4
	Blocks lateral surfaces	1.5	9.4	18.2
	Surfaces between blocks	98.1	89.1	80.4
	Sample support surfaces	0	0	0
	Vacuum vessel	0	0	0
Secondary Electrons (SE)	Blocks top surfaces	0	0	0
	Blocks lateral surfaces	3.5	19.7	86.9
	Surfaces between blocks	0.4	0.4	0
	Sample support surfaces	0	0	0
	Vacuum vessel	96.1	79.9	13.1
BackScattered Electrons (BSE)	Blocks top surfaces	0	0	0
	Blocks lateral surfaces	7.9	13.6	29.2
	Surfaces between blocks	1.3	7.0	1.5
	Sample support surfaces	0	0	0
	Vacuum vessel	90.8	79.4	69.3

SPIS simulations are being made for each samples presented on Fig. 6 and for other samples. Results depend on the primary electron energy and the magnetic field amplitude.

CONCLUSION

As a step toward understanding the effect of the magnetic field on the electron emission proprieties under electron impact, a new experimental setup has been developed. This setup is dedicated to measure the Total Electron Emission Yield under a magnetic field perpendicular to the sample surface. Thanks to measurements and PIC modeling we have validated the measurement methodology. First results show a decrease of the TEEY when the magnetic field is applied but we still need further investigations before drawing any final conclusion.

We are working on making new measurements and modeling with different magnetic field amplitudes as well as different morphology surface samples. We are investigating the correlations between surface morphology and magnetic field amplitude on electron emission properties.

REFERENCES

- [1] J. R. M. Vaughan, "Multipactor," Electron Devices, IEEE Trans., vol. 35, no. 7, pp. 1172–1180, 1988.
- [2] J. de Lara, F. Pérez, M. Alfonseca, L. Galán, I. Montero, E. Román, and D. R. Garcia-Baquero, "Multipactor prediction for on-board spacecraft RF equipment with the MEST software tool," *IEEE Trans. Plasma Sci.*, vol. 34, no. 2, pp. 476–484, 2006.
- [3] M. Goniche, C. El Mhari, M. Francisquez, S. Anza, J. H. Belo, P. Hertout, and J. Hillairet, "Modelling of power limit in RF antenna waveguides operated in the lower hybrid range of frequency," *Nucl. Fusion*, vol. 54, no. 1, p. 13003, 2014.
- [4] G. Rumolo, F. Ruggiero, and F. Zimmermann, "Simulation of the electron-cloud build up and its consequences on heat load, beam stability, and diagnostics," *Phys. Rev. Spec. Top. Accel. Beams*, vol. 4, no. 1, pp. 25–36, 2001
- [5] R. Udiljak, D. Anderson, P. Ingvarson, U. Jordan, U. Jostell, L. Lapierre, G. Li, M. Lisak, J. Puech, and J. Sombrin, "New method for detection of multipaction," *IEEE Trans. Plasma Sci.*, vol. 31, no. 3, pp. 396–404, 2003.
- [6] A. Al-mudhafar, P. Jerome, and H. Hartnagel, "Investigation of Multipactor Effect in Satellite Components Using CST Particle in Cell Solver," *Proc. MULCOPIM 2014*, no. 1.
- [7] G. Romanov, "Update on multipactoring in coaxial waveguides using {CST} Particle Studio," 2011.
- [8] V. E. Semenov, E. I. Rakova, D. Anderson, M. Lisak, and J. Puech, "Multipactor in rectangular waveguides," *Phys. Plasmas*, vol. 14, no. 3, pp. 1–8, 2007.
- [9] S. Anza, T. Pinheiro, J. Armendáriz, F. J. Pérez, M. Rodríguez, and C. Gahete, "Recent Developments on FEST3D / SPARK3D simulation tools," *Int. Work. Multipactor, Corona Passiv. Intermodulation Sp. RF Hardw.*, vol. 6, no. 1, pp. 1–5, 2011.
- [10] A. Valfells, L. K. Ang, Y. Y. Lau, and R. M. Gilgenbach, "Effects of an external magnetic field, and of oblique radio-frequency electric fields on multipactor discharge on a dielectric," *Phys. Plasmas*, vol. 7, no. 2, p. 750, 2000
- [11] M. Rosler, "Theory of Electron Emission from Solids by Proton and Electron Bombardment," vol. 213, pp. 213–226, 1988.
- [12] J. F. Roussel, F. Rogier, D. Volpert, G. Dufour, J. C. Matéo-Vélez, J. Forest, and A. Hilgers, "Spacecraft Plasma Interaction Software (SPIS): Numerical Solvers Methods and Architecture," *JAXA Spec. Publ.*, vol. JAXA-SP-05, pp. 462–472, 2005.
- [13] M. Belhaj, O. Jbara, M. Filippov, E. Rau, and M. Andrianov, "Analysis of two methods of measurement of surface potential of insulators in SEM: electron spectroscopy and X-ray spectroscopy methods," *Appl. Surf. Sci.*, vol. 177, no. 1–2, pp. 58–65, 2001.
- [14] T. Tondu, M. Belhaj, and V. Inguimbert, "Methods for measurement of electron emission yield under low energy electron-irradiation by collector method and Kelvin probe method," *J. Vac. Sci. Technol. A Vacuum, Surfaces, Film.*, vol. 28, no. 5, p. 1122, 2010.
- [15] I. Katz, D. E. Parks, M. J. Mandell, J. M. Harvey, D. H. Brownell Jr., S. S. Wang, and M. Rotenberg, "A three dimensional dynamic study of electrostatic charging in materials," *Soc. Stud. Sci.*, vol. 3367, no. NASA CR-135256, p. 342, 1977.
- [16] R. E. Kirby and F. K. King, "Secondary electron emission yields from PEP-II accelerator materials," *Nucl. Instruments Methods Phys. Res. Sect. A Accel. Spectrometers, Detect. Assoc. Equip.*, vol. 469, no. 1, pp. 1–12, 2001.
- [17] P. Kumar, C. Watts, T. Svimonishvili, M. Gilmore, and E. Schamiloglu, "The Dose Effect in Secondary Electron Emission," *IEEE Trans. Plasma Sci.*, vol. 37, no. 8, pp. 1537–1551, 2009.
- [18] L. Wang, T. Raubenheimer, G. Stupakov, and M. Park, "SUPPRESSION OF SECONDARY EMISSION IN A MAGNETIC FIELD USING A SAWTOOTH AND ISOSCELES TRIANGLE SURFACE," in *Proceedings of EPAC 2006, Edinburgh, Scotland*, 2006, no. August, pp. 897–899.
- [19] C. Chang, G. Liu, C. Tang, C. Chen, and J. Fang, "Review of recent theories and experiments for improving high-power microwave window breakdown thresholds," *Phys. Plasmas*, vol. 18, no. 5, 2011.